JSHC
Japan Society of Histochemistry and Cytochemistry
Established 1959

Acta Histochem. Cytochem. 42 (6): 159–169, 2009
doi:10.1267/ahc.09023

Immunohistochemical Localization of the Aquaporins AQP1, AQP3, AQP4, and AQP5 in the Mouse Respiratory System

Toshiyuki Matsuzaki[1,2], Hidekazu Hata[1], Hitoshi Ozawa[2] and Kuniaki Takata[3]

[1]Institute of Experimental Animal Research, Gunma University Graduate School of Medicine, Maebashi, Gunma 371–8511, Japan, [2]Department of Anatomy and Neurobiology, Nippon Medical School Graduate School of Medicine, Bunkyo-ku, Tokyo 113–8602, Japan and [3]Department of Anatomy and Cell Biology, Gunma University Graduate School of Medicine, Maebashi, Gunma 371–8511, Japan

Received August 24, 2009; accepted August 31, 2009; published online November 3, 2009

Aquaporins are membrane water channel proteins that function mainly in water transfer across cellular membranes. In our present study, we investigated the immunohistochemical distribution of aquaporin 1 (AQP1), AQP3, AQP4, and AQP5 in the mouse respiratory system by immunofluorescence, immunoperoxidase, and immunoelectron microscopy. AQP3, AQP4, and AQP5 are expressed in epithelial cells, whereas AQP1 is expressed in subepithelial connective tissues and capillaries. In the airway surface epithelia from the nasal cavity to the intrapulmonary bronchioles, AQP5 was found to be mainly localized to the luminal side and both AQP3 and AQP4 to the abluminal side. In the alveolar epithelium, AQP5 is localized to the apical membranes of both type I and type II alveolar cells. Compared with the previous studies on the rat respiratory system, in which AQP5 is restricted to the alveolar type I cells and absent from the airway surface epithelia, we found that AQP5 in the mouse is much more widely distributed throughout the surface epithelia. These results suggest that AQP5 has a critical role in water-handling, such as the maintenance of airway surface liquid and clearance of alveolar fluid in the mouse respiratory system.

Key words: water channel, aquaporin (AQP), mouse, respiratory system, immunohistochemistry

I. Introduction

Cells are enclosed by a plasma membrane through which water permeates slowly by simple diffusion. Some cell types, such as renal collecting duct cells, also permeate a larger quantity of water and in these cases the membrane water channel known as aquaporin (AQP) serves as the molecular machinery for such rapid and efficient transfer through the membrane, as first described by Agre and colleagues in 1992 [23]. Thus far, 13 AQP isoforms (AQP0–AQP12) have been identified in mammals [10, 14, 26] and are classified into three groups as follows: 1) the classical aquaporins (AQP1, AQP2, AQP4, and AQP5) which are water selective channels; 2) the aquaglyceroporins (AQP3, AQP7, AQP9, and AQP10) which also permeate small solutes such as glycerol and urea; and 3) unorthodox aquaporins (AQP6, AQP8, AQP11, and AQP12), whose function remains unknown. Each isoform is expressed in a tissue-specific manner and is also distributed in a specific domain of the cells in question [27]. We have raised specific antibodies to each AQP isoform in our laboratory and revealed the corresponding distributions in several tissues and organs [1, 2, 12, 13, 15–17, 19]. These data are fundamental to our understanding of the physiological roles of the aquaporins in each tissue and/or cell.

In our present study, we focused on the mouse respiratory system. The distributions of AQP1, AQP3, AQP4, and AQP5 have now been reported in the rat respiratory system [13, 20]. However, the comprehensive study in the mouse respiratory system has yet to be done. Since the mouse is commonly used in the genetic and physiological studies and

Correspondence to: Toshiyuki Matsuzaki, M.D., Ph.D, Department of Anatomy and Neurobiology, Nippon Medical School Graduate School of Medicine, 1–1–5 Sendagi, Bunkyo-ku, Tokyo 113–8602, Japan.
E-mail: matoshi@nms.ac.jp

the histological architecture of the mouse tracheal epithelium is markedly different from that in other species [7, 21, 22], we examined the comprehensive and detailed localization of aquaporins in the mouse respiratory system by immunofluorescence, immunoperoxidase, and immunoelectron microscopy and compared it with the results in the rat.

The expression and distribution of AQP3, AQP4, and AQP1 in the mouse is basically equivalent to that in rat but we found that AQP5 in the mouse localizes to the luminal side of the surface epithelium throughout the airway as well as in both type I and type II alveolar cells, whereas it has been shown to be restricted to the alveolar type I cells and to be absent from any other surface epithelium in the rat [20]. These results suggest that AQP5 could play more significant roles in water-handling such as maintenance of airway surface liquid and clearance of alveolar fluid in the mouse respiratory epithelium in comparison with the rat.

II. Materials and Methods

Antibodies

The anti-AQP antibodies used in this study have been raised in our laboratory and shown to be specific to each isoform as listed in Table 1. Goat anti-surfactant protein A (SP-A) antibody was purchased from Santa Cruz Biotechnology (sc-7700; Santa Cruz, CA).

Animal and tissue preparation

ICR mice were obtained from Japan SLC (Shizuoka, Japan) and maintained on normal chow. Male and female 8- to 12-week-old mice were used in this study. The animals were deeply anesthetized with an intraperitoneal injection of a mixture of ketamine (100 mg/kg) and xylazine (10 mg/kg) and killed by cervical dislocation or perfusion fixation. Fresh unfixed tissues were prepared to survey the distribution of aquaporins by light microscopy. They were quickly embedded in Tissue-Tek OCT compound (Sakura Finetechnical, Tokyo, Japan), frozen in liquid nitrogen, and stored at –80°C until use. Perfusion fixation of the tissues was carried out to enable detailed localization analysis by both electron and light microscopy. The fixatives used were 4% paraformaldehyde in 0.1 M sodium phosphate buffer (pH 7.4), or 4% paraformaldehyde in 0.1 M sodium cacodylate buffer (pH 7.4) containing 25 mM $CaCl_2$ [29]. After perfusion, the tissues were removed and fixed in the same fixative overnight at 4°C. To prepare paraffin sections, tissues were dehydrated through a graded ethanol series and embedded in paraffin. To prepare cryostat sections, tissues were immersed in 30% sucrose in phosphate-buffered saline (PBS), embedded in Tissue-Tek OCT compound, frozen in liquid nitrogen, and stored at −80°C until use. All animal experiments were performed in compliance with the NIH Guide for the Care and Use of Laboratory Animals and approved by the Animal Care and Experimentation Committee, Gunma University, Showa Campus (admission no. 7–99).

Table 1. *List of the anti-aquaporin antibodies used in this study*

Isoform	Antibody Name	Details	References
AQP1	AffRaTM31	Affinity-purified rabbit anti-AQP1	[17]
	AffGPTM31	Affinity-purified guinea pig anti-AQP1	[17]
AQP2	AffRaTM11	Affinity-purified rabbit anti-AQP2	[25]
AQP3	AffRaTM5	Affinity-purified rabbit anti-AQP3	[13]
	AffGPTM5b	Affinity-purified guinea pig anti-AQP3	[17]
AQP4	AffRaTM13	Affinity-purified rabbit anti-AQP4	[1]
AQP5	AffRaTM14	Affinity-purified rabbit anti-AQP5	[12]
	AffRaTM41	Affinity-purified rabbit anti-AQP5	[18]
	AffGPTM41	Affinity-purified guinea pig anti-AQP5	[18]

Immunohistochemistry for examination by light microscopy

To survey the distribution of aquaporins, unfixed frozen tissues were sectioned with a cryostat, mounted on MAS-coated glass slides (Matsunami, Osaka, Japan), and immersed in ethanol for 30 min at −20°C. After washing with PBS, these samples were processed for indirect immunofluorescence labeling.

To examine the detailed localization of the aquaporins, cryostat sections or paraffin sections from formaldehyde-fixed tissues were cut and mounted on MAS-coated glass slides. The paraffin sections were then deparaffinized and rehydrated. The specimens were then immersed in 20 mM Tris-HCl, pH 9.0, and antigen retrieval was performed by autoclaving for 10 min at 110°C or heating microwave for 30 min. The slides were then processed for either indirect immunoperoxidase or immunofluorescence labeling.

For immunoperoxidase labeling, endogenous peroxidase activity was blocked by 0.5% H_2O_2 in methanol for 30 min at room temperature. The non-specific binding of antibodies was blocked by incubating with PBS containing 1% bovine serum albumin (BSA). The samples were then sequentially incubated with primary antibodies diluted in PBS containing 1% BSA overnight at 4°C followed by horseradish peroxidase-coupled goat anti-rabbit antibodies (P0448, DAKO, diluted in 1:100). DAB reactions were performed using a liquid DAB+ system (K3467, DAKO) after which the sections were stained with hematoxylin, washed with running water, dehydrated in a graded series of ethanol and xylene, and then mounted with Permount (Fisher Scientific, Fair Lawn, NJ).

For immunofluorescence labeling, the non-specific binding of antibodies was also blocked by incubating with PBS containing 1% BSA. The slides were then sequentially incubated with primary antibodies diluted in PBS containing 1% BSA overnight at 4°C and fluorescently labeled secondary antibodies for 90 min at room temperature. The fluorescently labeled secondary antibodies used were 1) Rhodamine Red-X-conjugated donkey anti-rabbit IgG (Jackson Immunoresearch, West Grove, PA), 2) Rhodamine Red-X-conjugated donkey anti-guinea pig IgG (Jackson

Immunoresearch), 3) AlexaFluor 488-conjugated donkey anti-rabbit IgG (Invitrogen, Carlsbad, CA), 4) fluorescein isothiocyanate (FITC)-conjugated donkey anti-guinea pig IgG (Jackson Immunoresearch), and 5) AlexaFluor 488-conjugated donkey anti-goat IgG (Invitrogen) [24]. For nuclear counterstaining, 4',6-diamidino-2-phenylindole (DAPI) was added to the mixture of secondary antibodies [24]. Specimens were mounted with Vectashield (Vector Laboratories, Burlingame, CA)

Peroxidase-labeled specimens were observed with an AX-80 microscope (Olympus, Tokyo, Japan). Fluorescence-labeled specimens were observed with a BX-62 or an AX-80 microscope equipped with Nomarski differential interference-contrast and epifluorescence optics (Olympus), or with a FV-1000 laser confocal microscope (Olympus).

Immunoelectron microscopy

Immunoperoxidase-labeled specimens were prepared using the same procedure described for light microscopy. After the DAB reaction, sections were refixed with 2.5% glutaraldehyde in 0.1 M cacodylate buffer, pH 7.4, for 10 min, washed with water, and covered with 1% osmium tetroxide in 0.1 M cacodylate buffer, pH 7.4, for 15 min. The slides were then rinsed with water, dehydrated in a graded series of ethanol, and embedded in epoxy resin. Ultrathin sections were then cut and examined with a JEM-1010 electron microscope (JEOL, Tokyo, Japan).

Histochemical controls

The specificity of immunostaining was verified by preincubating the AQP antibodies with the peptide (10–50 μg/ml) originally used as the immunogen and also by omitting the primary antibodies from the first incubation step.

III. Results

Distribution of aquaporins in the mouse respiratory tract

We first surveyed the distribution of AQP1, AQP2, AQP3, AQP4, and AQP5 using sagittal sections of tissues sampled from the head and neck regions which contain the oral cavity, nasal cavity, pharynx, larynx, upper part of the trachea, as well as the upper part of the esophagus. To preserve antigenicity, cryostat sections from unfixed tissues were fixed with ethanol and processed for immunofluorescence microscopy. When these specimens were examined at lower magnification, labeling for AQP1, AQP3, AQP4, and AQP5 was detectable. AQP3, AQP4, and AQP5 signals were evident in the epithelium, whereas AQP1 was found to be expressed in the subepithelial tissues and capillaries. No labeling for AQP2 was detected. We surveyed both male and female mice and found no apparent difference in the expression and distribution of these isoforms.

1) Localization of AQP3, AQP4, and AQP5

AQP3 was found to be continuously distributed throughout the respiratory and digestive tract epithelia in the mouse tissue sections examined (Fig. 1A), as previously shown in the rat [13]. In contrast however, both AQP4 and AQP5 were found to be restricted to the respiratory tract epithelium (Fig. 1B, C). The types of epithelial tissues in these areas are either stratified squamous epithelium in the posterior part of the nasal cavity, pharynx, and some parts of the larynx, or pseudostratified columnar epithelium in other parts of larynx and in the trachea. Strong staining of AQP4 was observed in the pseudostratified columnar epithelium of the posterior surface of the epiglottis and the trachea (Fig. 1B). Strong AQP5 expression was found to be distributed throughout the respiratory tract epithelia, i.e. both in the stratified squamous and pseudostratified columnar epithelia of the nasal cavity, pharynx, larynx, and trachea (Fig. 1C).

In the stratified squamous epithelium, strong AQP3 and AQP5 expression was evident. When we then examined at a higher magnification the stratified squamous epithelium that had been double-labeled for AQP3 and AQP5, AQP3 staining was present in the basal and intermediate layers (Fig. 1D1), whereas AQP5 expression was detected in the intermediate and surface layers (Fig. 1D2). In the pseudostratified columnar epithelium, AQP3, AQP4, and AQP5 were all found to be abundantly expressed. Since it is not easy to maintain the structure of the pseudostratified columnar epithelium in fresh-frozen specimens, detailed AQP localization analyses in this tissue were performed using formaldehyde-fixed tracheal specimens subjected to antigen retrieval [18, 29]. Intense staining for AQP3 was found in the membranes of the basal cells and also in a small number of non-ciliated columnar cells, in which the localization of this isoform is restricted to the basolateral membranes (Fig. 2A). To further characterize the AQP3-positive non-ciliated columnar cells, immunoelectron microscopy was carried out. AQP3-positive cells appeared to be mucous cells in appearance as they contain electron-lucent secretory granules (data not shown). However, we could not identify this cell type more precisely since the number of AQP3-positive cells was very low. AQP4 was found to be present in the plasma membranes of the basal cells and the basolateral membranes of the columnar cells (Fig. 2A). In contrast to AQP3, AQP4 appeared to be expressed in all ciliated and non-ciliated columnar cells (Fig. 2A).

Intense staining for AQP5 was evident in the apical surfaces in a discontinuous pattern. When we carefully examined these specimens at a higher magnification, AQP5 localization was found to be restricted to the non-ciliated surfaces (Fig. 2B). In addition to its strong labeling in the apical membranes, the basolateral membranes of non-ciliated cells in addition to the cell membranes of basal cells were AQP5-positive (Fig. 2B). The ultrastructural localization of AQP5 was then confirmed by immunoelectron microscopy (Fig. 3). Labeling for this isoform at the luminal surface was found to be restricted to the apical membranes of non-ciliated cells and no staining was evident in ciliated cells (Fig. 3). According to previous studies, non-ciliated cells of the mouse tracheal epithelium can be classified into different types [21, 22]. It appears from our current observa-

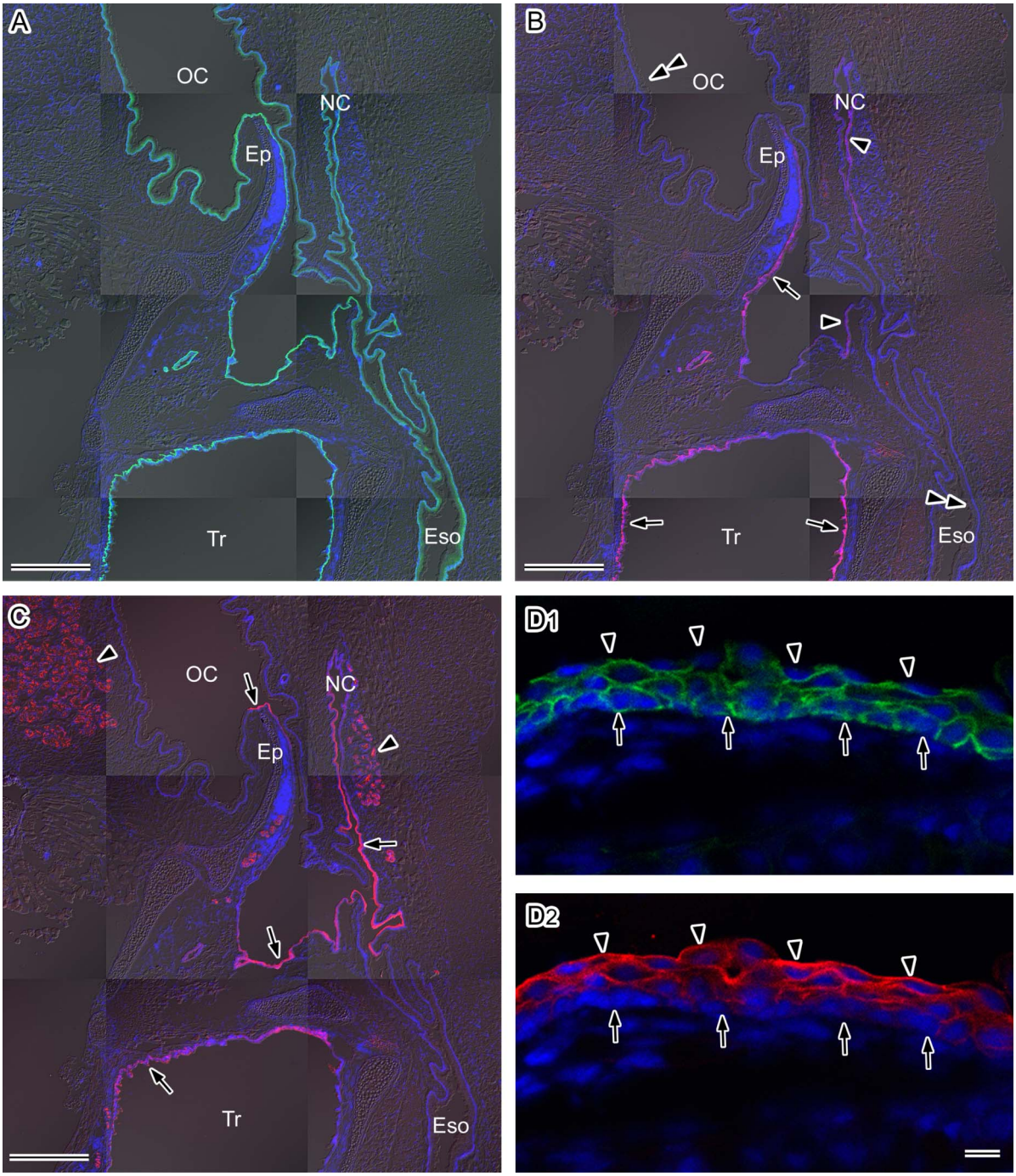

Fig. 1. Distribution of AQP3, AQP4, and AQP5 in the mouse upper respiratory tract. Sagittal sections of the head and neck region of the mouse were cut with a cryostat, fixed with ethanol, and then subjected to immunofluorescence microscopy. Nuclear DNA was counterstained with DAPI (blue). **A–C:** Lower magnification views of AQP3 (green in **A**), AQP4 (red in **B**), and AQP5 (red in **C**). Fluorescence images merged with the corresponding Nomarski images are shown. OC, oral cavity; NC, nasal cavity; Ep, epiglottis; Eso, esophagus; Tr, trachea. **A:** AQP3 is distributed throughout the respiratory and digestive tract epithelia. **B:** AQP4 is restricted to the respiratory tract epithelium. Strong fluorescent immunostaining is evident in the posterior surface of the epiglottis and trachea (arrows). Weak staining is detectable in the nasal cavity and pharynx (arrowheads). No labeling is found in the oral cavity or esophagus (double-arrowheads). **C:** AQP5 expression is restricted to the respiratory tract epithelium and the glands (arrowheads). Strong immunolabeling is found in a part of the epiglottis, nasal cavity, pharynx, larynx, and trachea (arrows). **D:** Higher magnification views of the stratified squamous epithelium of the epiglottis double-stained for AQP3 (green in **D1**) and AQP5 (red in **D2**) under a laser confocal microscope. AQP3 is abundant in the basal and intermediate layers, whereas AQP5 is abundant in the intermediate and surface layers. The base and luminal surface of the epithelium are indicated by arrows and arrowheads, respectively. Bars=50 μm (**A–C**), 10 μm (**D**).

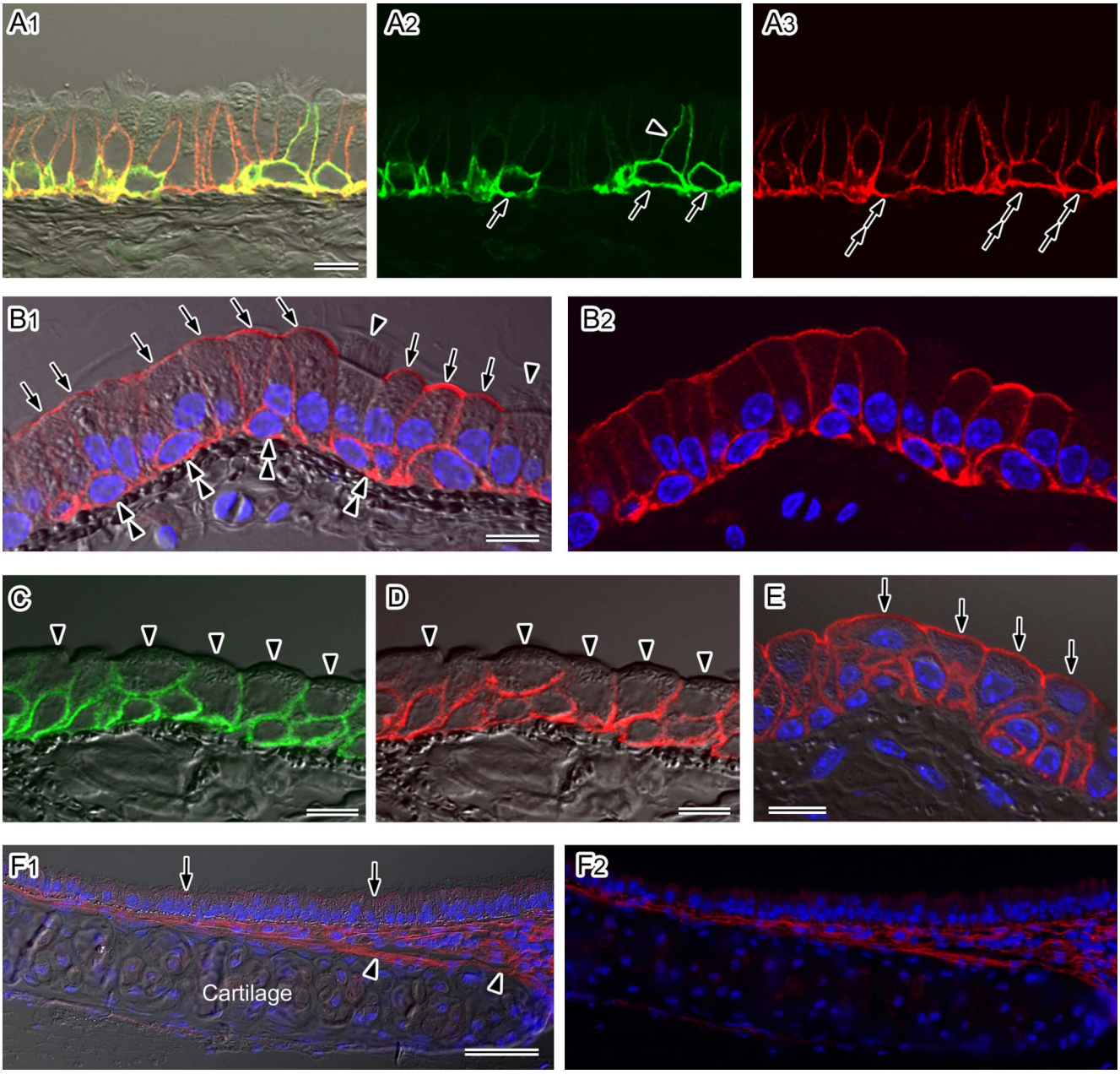

Fig. 2. Localization of AQP1, AQP3, AQP4, and AQP5 in the mouse trachea. Cryostat sections (**A–D**) or paraffin sections (**E** and **F**) were analyzed by immunofluorescence microscopy after antigen retrieval. Nuclear DNA was counterstained with DAPI (blue in **B, E**, and **F**). **A–E:** Higher magnification views observed under a laser confocal microscope. Fluorescence images merged with (**A1, B1, C, D**, and **E**) or without (**A2, A3**, and **B2**) the corresponding Nomarski images are shown. **A:** Double-labeling for AQP3 (green) and AQP4 (red) in the pseudostratified columnar epithelium. Strong AQP3 staining is evident at the cell membranes of basal cells (arrows). A sub-population of the non-ciliated columnar cells is AQP3-positive on their basolateral membranes (arrowhead). AQP4 expression is evident in all basal (double-arrows) and columnar cells. In the columnar cells, AQP4 staining is restricted to the basolateral membranes. **B:** AQP5 staining (red) in the pseudostratified columnar epithelium. Strong signals are localized to the apical membranes of non-ciliated columnar cells (arrows). The basolateral membranes of the non-ciliated cells and cell membranes of the basal cells (double-arrowheads) are also AQP5-positive. No AQP5 signals are evident in ciliated columnar cells (arrowheads). **C–E:** The stratified cuboidal epithelium of the trachea was immunostained for AQP3 (green in **C**), AQP4 (red in **D**), and AQP5 (red in **E**). AQP3 and AQP4 signals are evident in all layers except for the luminal membranes of the surface cells (arrowheads). AQP5 is also expressed in all layers including the luminal membranes of non-ciliated surface cells (arrows). **F:** AQP1 staining (red) observed under low magnification with a conventional fluorescence microscope. Fluorescence images merged with (**F1**) or without (**F2**) a corresponding Nomarski image are shown. AQP1 staining is evident in the subepithelial connective tissues including the perichondrium (arrowheads). No signals for this isoform are found in the epithelium (arrows). Bars=50 μm (**A**), 10 μm (**B–F**).

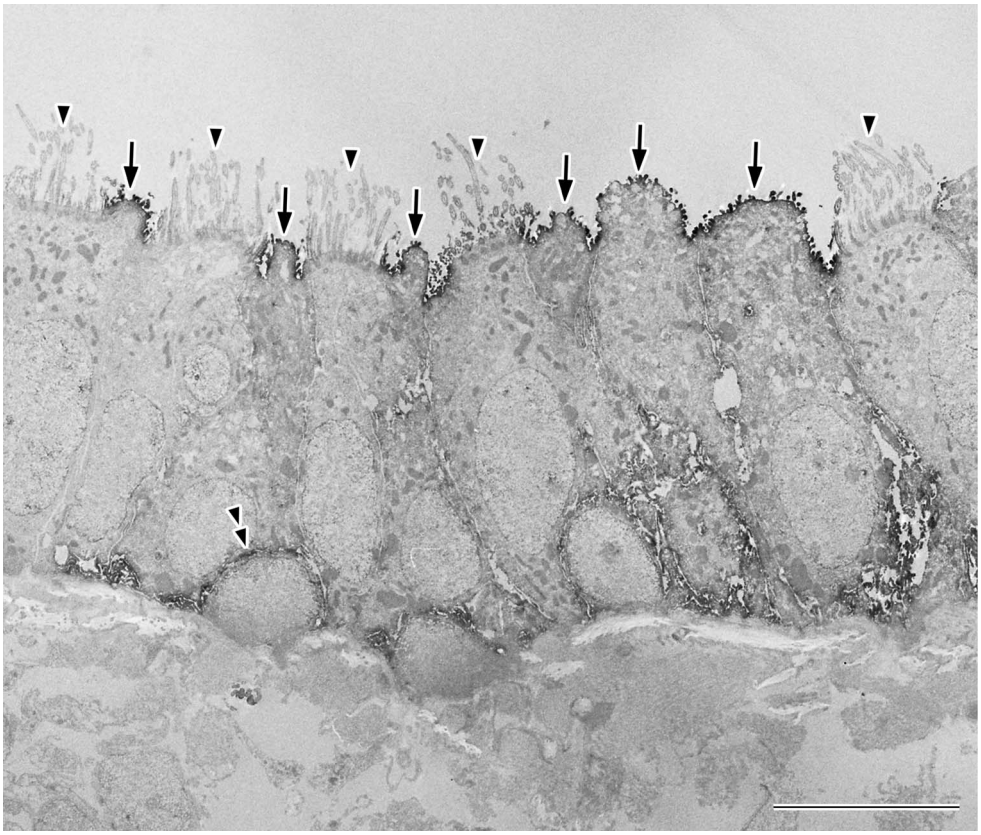

Fig. 3. Ultrastructural localization of AQP5 in the mouse tracheal epithelium. AQP5 is localized to the apical membrane of the non-ciliated columnar cells (arrows). The cell membranes of the basal cells are also found to be positive (double-arrowhead). No signals are evident in the apical membranes of the ciliated columnar cells (arrowheads). Bar=10 μm.

tions that all types of non-ciliated cells are AQP5-positive, although we cannot easily classify these cell types at this stage. In addition to the non-ciliated cells, the localization of AQP5 at the plasma membranes of basal cells was also confirmed by our immunoelectron microscopy (Fig. 3).

When we next examined a number of tracheal sections, a transitional type of epithelium, such as a stratified cuboidal epithelium, was sometimes evident. As shown in Figure 2C–E, a stratified cuboidal epithelium covered with non-ciliated cells on its surface could be observed. AQP3 (Fig. 2C) and AQP4 (Fig. 2D) were found to be expressed in all layers from the basal to the surface with the exception of the apical membranes of the superficial layer. AQP5 was also detected in all layers from the basal to the surface including the apical membranes of the superficial layer (Fig. 2E).

2) Localization of AQP1

As is the case for many tissues, AQP1 was detected in the capillaries. In addition, AQP1 was found to be distributed in the subepithelial connective tissue of the mouse respiratory tract (Fig. 2F), as previously shown in the rat [20], but not detected in the subepithelial connective tissue of the oral cavity or esophagus of the mouse.

Distribution of aquaporins in the lung

The distribution of aquaporins in the mouse lung was examined using formaldehyde-fixed specimens subjected to antigen retrieval. Positive labeling for AQP1, AQP3, AQP4, and AQP5 was observed.

1) Intrapulmonary bronchioles

AQP3, AQP4, and AQP5 were found to be expressed in the intrapulmonary bronchiolar epithelium, which is a simple columnar or cuboidal epithelium. AQP3 staining was evident in a small number of non-ciliated but ciliated cells in the proximal part of the bronchioles, in which its labeling was restricted to the basolateral membranes (Fig. 4A). The number of AQP3-positive cells was observed to decrease nearer to the alveoli, with no staining for this isoform evident in the alveoli. In contrast to AQP3, intense staining for AQP4 was evident in all epithelial cells throughout the bronchioles, where it was found to be restricted to the basolateral membranes (Fig. 4B). AQP4 labeling again became weaker nearer the alveoli and was absent in the alveoli. AQP5 was stained positively in non-ciliated epithelial cells in the bronchioles towards the alveoli (Fig. 4C). This labeling was mainly present in the apical membranes, although weak staining for AQP5 was also evident in the basolateral membranes. Apical labeling for AQP5 was found to be leading

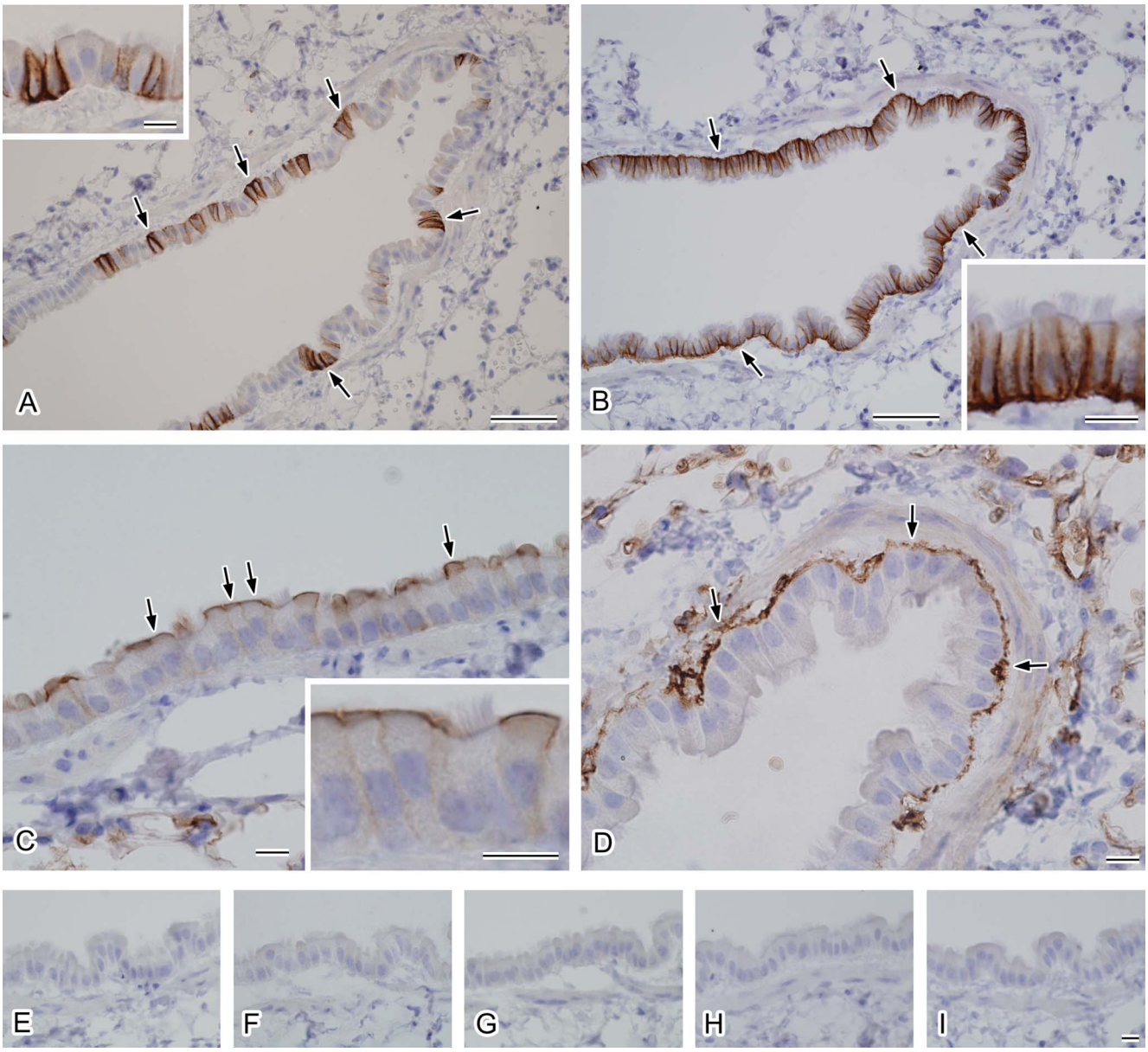

Fig. 4. Localization of AQP1, AQP3, AQP4, and AQP5 in the mouse intrapulmonary bronchioles. Cryostat sections of the mouse lung were subjected to indirect immunoperoxidase labeling for AQP3 (**A**), AQP4 (**B**), AQP5 (**C**), and AQP1 (**D**) after antigen retrieval. **A:** Labeling for AQP3 is localized to the basolateral membranes of a portion of the columnar cells (arrows). A higher magnification view of the epithelial cells is shown (inset). **B:** AQP4 is localized to the basolateral membranes of all columnar cells (arrows). A higher magnification view of the epithelial cells is shown (inset). **C:** AQP5 is localized to the apical membranes of non-ciliated columnar cells (arrows). A higher magnification view of the epithelial cells is shown (inset). **D:** AQP1 staining is evident in the subepithelial connective tissues (arrows). **E–I:** Histochemical controls. The primary antibody incubation was omitted (**E**) or each primary antibody (**F**, AQP3; **G**, AQP4; **H**, AQP5; and **I**, AQP1) was preabsorbed with each antigen peptide. Bars=50 μm (**A** and **B**), 10 μm (**C** and **D**), 10 μm (insets), 10 μm (**E–I**).

toward the alveolar surface. In contrast to the distribution of AQP3, AQP4, and AQP5 in epithelial cells, AQP1 was found to be present in the subepithelial connective tissues in a pattern similar to that in the trachea (Fig. 4D).

2) Alveoli

In the alveolar areas of the mouse tissues, AQP1 and AQP5 were both found to be expressed. Double-labeling for AQP1 and AQP5 also clearly showed that these isoforms are restricted to the capillary endothelium and to the alveolar surface epithelium, respectively (Fig. 5A). There are two types of alveolar cells, namely type I and type II, and when we carefully observed AQP5 localization in the mouse alveoli, the alveolar surface was found to be continuously

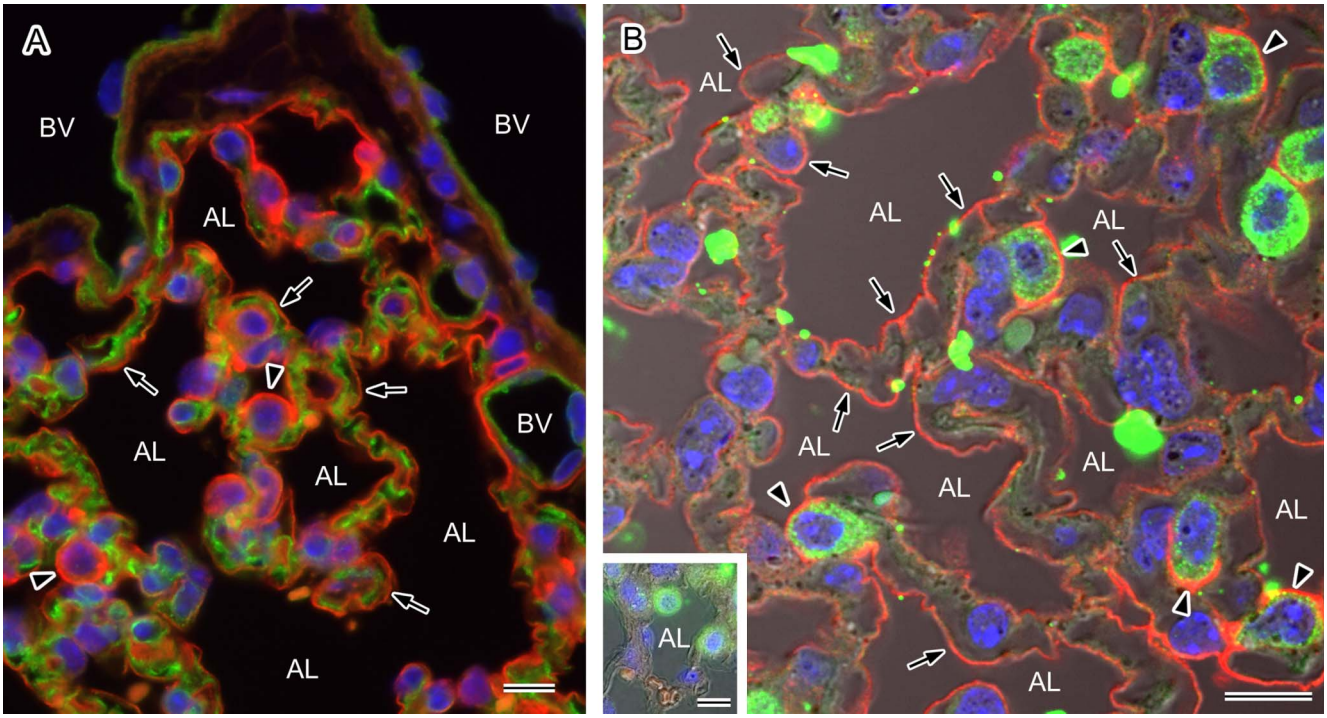

Fig. 5. Localization of AQP1 and AQP5 in the mouse alveoli. Paraffin sections of the mouse lung were analyzed by immunofluorescence microscopy after antigen retrieval for the localization of AQP1 and AQP5. Nuclear DNA was counterstained with DAPI (blue). **A:** Double staining for AQP1 (green) and AQP5 (red) observed under a low magnification with a conventional microscope. AQP1 and AQP5 staining can be seen on the vascular side and at the alveolar surface (arrows), respectively. The entire alveolar surface is positive for AQP5 and strong expression of this isoform can be seen in the protruding cells (arrowheads). BV, blood vessel; AL, alveolar lumen. **B:** Double staining for AQP5 (red) and the type II cell marker SP-A (green) observed under high magnification with a laser confocal microscope. A fluorescent image merged with a corresponding Nomarski image is shown. The entire luminal surface is positive for AQP5 (arrows) and stronger signals for this isoform are evident at the apical membranes of SP-A-positive type II alveolar cells (arrowheads). Positive labeling for AQP5 is abolished in the presence of the antigen peptide (inset). AL, alveolar lumen. Bars=10 μm.

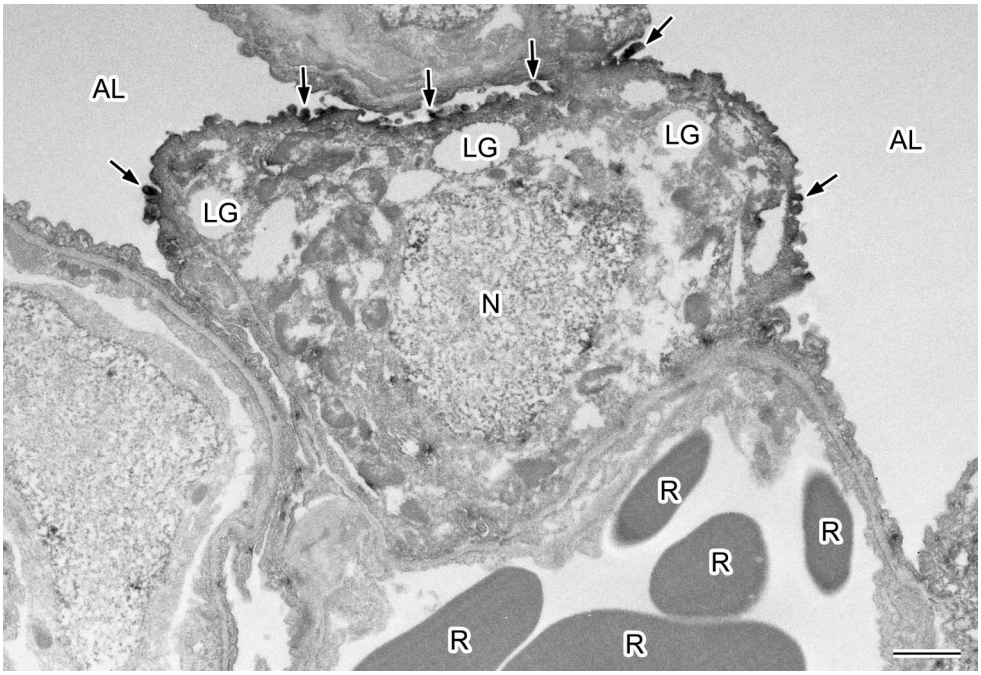

Fig. 6. Ultrastructural localization of AQP5 in the mouse type II alveolar cell. AQP5 is localized at the apical membrane of the type II alveolar cell (arrows) containing lamellar granules (LG) in the cytoplasm and microvilli on their apical surface (arrows). N, nucleus; AL, alveolar lumen; R, red blood cells. Bar=1 μm.

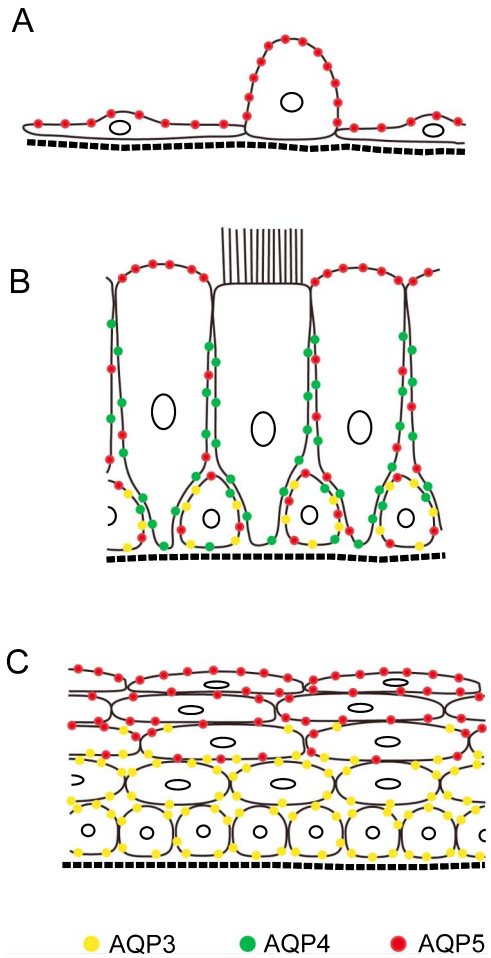

Fig. 7. Schema summarizing the distribution patterns of AQP3, AQP4, and AQP5 in the mouse respiratory epithelia. **A:** Alveolar epithelium containing exquisitely thin type I and a cuboidal type II cells. **B:** Tracheal pseudostratified columnar epithelium composed of ciliated, non-ciliated, and basal cells. **C:** Stratified squamous epithelium in the upper airway.

labeled with more intense positivity in the cells protruding to the lumen. These strongly stained cells appeared by morphology to be type II but to confirm this we performed double-labeling for AQP5 and a type II cell marker, SP-A [3]. AQP5 was found to be present in both SP-A-negative type I and SP-A-positive type II alveolar cells (Fig. 5B). More intense labeling was evident in the type II cells compared with the type I cells. We also performed immunoelectron microscopy and found clear localization of AQP5 to the apical membranes of cells harboring lamellar granules in their cytoplasm and microvilli on their apical surface, i.e. type II cells (Fig. 6), as well as type I cells.

3) Visceral pleura

Strong staining for AQP1 was found in the mesothelial cells of the visceral pleura (data not shown) as previously shown also in the rat [20].

Histochemical controls

Positive labeling for the aquaporin isoforms described in this study was abolished when each primary antibody was preabsorbed with the antigen peptide or when the primary antibody incubation was omitted (Fig. 4E–I and Fig. 5B).

IV. Discussion

In our present study, we examined the detailed distribution of aquaporins in the mouse respiratory system and our overall results are schematically summarized in Figure 7. The distributions of AQP1, AQP3, and AQP4 were found to be essentially similar to those previously reported in the rat [13, 20]. However, our finding that AQP5 is much more widely distributed among the surface epithelia in the mouse compared with the rat has not been reported previously. AQP5 is localized to the luminal side of the surface epithelia throughout the mouse respiratory system, whereas it is restricted to the alveolar type I cells in the rat. This suggests the functional importance of AQP5 in the maintenance of the luminal environment in the mouse by allowing water transfer between the lumen and the epithelial cells.

Aquaporins in the alveolar epithelium

The alveolar epithelium is composed of two types of cells, namely type I and type II cells, and it is well established that the exquisitely thin type I cells and cuboidal type II cells play a major role in gas exchange and surfactant production, respectively. In addition, alveolar fluid clearance is also a fundamental role of these cells and ensures effective gas exchange. Transalveolar fluid transport is believed to follow osmotic gradients, such that fluid transport is secondary to solute transport [9]. Recent studies also indicate the functional importance of epithelial sodium channel (ENaC) and cystic fibrosis transmembrane conductance regulator (CFTR) in ion transport via the apical membranes of both type I and type II cells, which provides the driving force for water transfer [6, 9]. In our current report, we clearly show the abundant localization of AQP5 at the apical membranes of type II cells in addition to type I cells, which strongly suggests that both types of cells could be responsible for water uptake. In contrast, the route of water exit across the basolateral membranes remains elusive as no aquaporins have been found here.

A previous study of the rat respiratory system described the restricted localization of AQP5 in type I cells [20]. We have also examined the rat lung and confirmed the absence of AQP5 in the type II cells (data not shown). These results together suggest that type II cells in the mouse alveoli may participate in alveolar fluid clearance more effectively than these cells in the rat. However, it is also the case that AQP5 knockout mice do not show any impairment in clearing their alveolar fluid in a physiological manner, although their osmotic water permeability levels are reduced [11]. Further studies will be required to elucidate both the physiological and pathophysiological roles of AQP5 in alveolar fluid clearance.

Aquaporins in the tracheal pseudostratified columnar epithelium

The conducting airway epithelium is covered by a layer of liquid, known as the airway surface liquid, which consists of mucus and an underlying periciliary watery layer that enables the cilia to clear mucus [4, 28]. The airway surface liquid is mainly secreted by the submucosal glands as an isotonic fluid and its composition is controlled by the surface epithelial cells to render it hypotonic [4, 28]. The functional importance of Na^+ absorption via ENaC and Cl^- secretion via CFTR, as well as Cl^- secretion via the calcium-activated Cl^- channel (CaCC), in controlling the composition of the airway surface liquid has been suggested. However, a detailed mechanism, including the pathway of water movement, remains elusive [4, 28]. Our current finding of the presence of AQP5 in both the apical and basolateral membranes, as well as AQP4 in the basolateral membranes, of non-ciliated cells strongly suggests the contribution of non-ciliated cells to transcellular water transfer. In contrast to the abundant localization of AQP5 in the mouse tracheal epithelium, the rat tracheal epithelium shows no obvious distribution of any aquaporin isoforms in its apical membranes [20]. This difference might simply arise from the fact that the major population of the mouse tracheal epithelial cells comprises non-ciliated cells, whereas these cells are the minor population in the rat [7, 21, 22]. The mechanisms underlying water handling may therefore differ between the mouse and rat trachea.

Aquaporins in the upper airway stratified squamous epithelium

It is generally thought that the stratified squamous epithelium plays a protective role from its luminal environment against various stress insults such as mechanical and/or chemical stress. For example, one of the important functions of the skin epidermis is to protect against water loss caused by evaporation, which is ensured by the presence of the outermost keratinized stratum corneum [5]. In addition to this barrier to evaporation, we have previously shown that AQP3 is expressed in the basal and intermediate layers of the epidermis. We thus hypothesized that AQP3 has a protective role against epidermal dehydration by supplying water from the subepithelial tissue to epithelial cells [13]. This was further suggested by previous analyses of AQP3-deleted mice, in which glycerol and water content in the epidermis is reduced [8]. The stratified squamous epithelium of the upper airway is also thought to be exposed to a similar environment to the epidermis since it is close to the entrance of the airway. Hence, AQP3 in the basal and intermediate layers could supply water and/or glycerol from the subepithelial tissue to the epithelial cells. However, we found surprisingly that AQP5 is localized to the intermediate and surface layers, so that the surface of the epithelium is water-permeable. In addition to its protective role against certain stress conditions, we speculate that the stratified squamous epithelium of the upper airway might enable transepithelial water transfer via AQP3 and AQP5 and contribute to the maintenance of a luminal surface environment.

In summary, in our present study we investigated the distribution of AQP1, AQP3, AQP4, and AQP5 in the mouse respiratory system. AQP5 was found to be broadly distributed throughout the mouse respiratory surface epithelium, but was previously shown to be restricted to the alveolar type I cells and absent from airway surface epithelia of the rat respiratory system. The distribution of AQP3 and AQP4 in the mouse epithelium as well as AQP1 in the subepithelial tissues was basically similar to the rat. These results suggest the functional importance of luminal AQP5 in maintaining the airway surface liquid and clearance of alveolar fluid, at least in the mouse respiratory system.

V. Acknowledgments

We thank T Kakinuma for technical assistance. This work was supported in part by Grants-in-Aid for Scientific Research from the Ministry of Education, Culture, Sports, Science, and Technology of Japan.

VI. References

1. Ablimit, A., Matsuzaki, T., Tajika, Y., Aoki, T., Hagiwara, H. and Takata, K. (2006) Immunolocalization of water channel aquaporins in the nasal olfactory mucosa. *Arch. Histol. Cytol.* 69; 1–12.
2. Ablimit, A., Aoki, T., Matsuzaki, T., Suzuki, T., Hagiwara, H., Takami, S. and Takata, K. (2008) Immunolocalization of water channel aquaporins in the vomeronasal organ of the rat: Expression of AQP4 in neuronal sensory cells. *Chem. Senses* 33; 481–488.
3. Andreeva, A. V., Kutuzov, M. A. and Voyno-Yasenetskaya, T. A. (2007) Regulation of surfactant secretion in alveolar type II cells. *Am. J. Physiol. Lung Cell Mol. Physiol.* 293; L259–L271.
4. Chambers, L. A., Rollins, B. M. and Tarran, R. (2007) Liquid movement across the surface epithelium of large airways. *Respir. Physiol. Neurobiol.* 159; 256–270.
5. Ebling, F. J. G. (1992) Functions of the skin. In "Textbook of Dermatology", ed. by R. H. Champion, J. L. Burton and F. J. G. Ebling, Blackwell Scientific, Oxford, pp. 125–155.
6. Folkesson, H. G. and Matthay, M. A. (2006) Alveolar epithelial ion and fluid transport. *Am. J. Respir. Cell Mol. Biol.* 35; 10–19.
7. Hansell, M. M. and Moretti, R. L. (1969) Ultrastructure of the mouse tracheal epithelium. *J. Morph.* 128; 159–169.
8. Hara-Chikuma, M. and Verkman, A. S. (2005) Aquaporin-3 functions as a glycerol transporter in mammalian skin. *Biol. Cell* 97; 479–486.
9. Herzog, E. L., Brody, A. R., Colby, T. V., Mason, R. and Williams, M. C. (2008) Knowns and unknowns of the alveolus. *Proc. Am. Thorac. Soc.* 5; 778–782.
10. Ishibashi, K. (2006) Aquaporin subfamily with unusual NPA boxes. *Biochim. Biophys. Acta* 1758; 989–993.
11. Ma, T., Fukuda, N., Song, Y., Matthay, M. A. and Verkman, A. S. (2000) Lung fluid transport in aquaporin-5 knockout mice. *J. Clin. Invest.* 105; 93–100.
12. Matsuzaki, T., Suzuki, T., Koyama, H., Tanaka, S. and Takata, K. (1999) Aquaporin-5 (AQP5), a water channel protein, in the rat salivary and lacrimal glands: immunolocalization and effect of secretory stimulation. *Cell Tissue Res.* 295; 513–521.
13. Matsuzaki, T., Suzuki, T., Koyama, H., Tanaka, S. and Takata, K. (1999) Water channel protein AQP3 is present in epithelia exposed to the environment of possible water loss. *J. Histochem.*

Cytochem. 47; 1275–1286.
14. Matsuzaki, T., Tajika, Y., Tserentsoodol, N., Suzuki, T., Aoki, T., Hagiwara, H. and Takata, K. (2002) Aquaporins: a water channel family. *Anat. Sci. Int.* 77; 85–93.
15. Matsuzaki, T., Tajika, Y., Suzuki, T., Aoki, T., Hagiwara, H. and Takata, K. (2003) Immunolocalization of water channel, aquaporin-5 (AQP5) in the rat digestive system. *Arch. Histol. Cytol.* 66; 307–315.
16. Matsuzaki, T., Ablimit, A., Tajika, Y., Suzuki, T., Aoki, T., Hagiwara, H. and Takata, K. (2005) Water channel aquaporin 1 (AQP1) is present in the perineurium and perichondrium. *Acta Histochem. Cytochem.* 38; 37–42.
17. Matsuzaki, T., Machida, N., Tajika, Y., Ablimit, A., Suzuki, T., Aoki, T., Hagiwara, H. and Takata, K. (2005) Expression and immunolocalization of water-channel aquaporins in the rat and mouse mammary gland. *Histochem. Cell Biol.* 123; 501–512.
18. Matsuzaki, T., Ablimit, A., Suzuki, T., Aoki, T., Hagiwara, H. and Takata, K. (2006) Changes of aquaporin 5-distribution during release and reaccumulation of secretory granules in isoproterenol-treated mouse parotid gland. *J. Electron Microsc.* 55; 183–189.
19. Morishita, Y., Matsuzaki, T., Hara-Chikuma, M., Andoo, A., Shimono, M., Matsuki, A., Kobayashi, K., Ikeda, M., Yamamoto, T., Verkman, A., Kusano, E., Ookawara, S., Takata, K., Sasaki, S. and Ishibashi, K. (2005) Disruption of aquaporin-11 produces polycystic kidneys following vacuolization of the proximal tubule. *Mol. Cell. Biol.* 25; 7770–7779.
20. Nielsen, S., King, L. S., Christensen, B. M. and Agre, P. (1997) Aquaporins in complex tissues. II. Subcellular distribution in respiratory and glandular tissues of rat. *Am. J. Physiol. Cell Physiol.* 273; C1549–C1561.
21. Pack, R. J., Al-Ugaily, L. H., Morris, G. and Widdicombe, J. G. (1980) The distribution and structure of cells in the tracheal epithelium of the mouse. *Cell Tissue Res.* 208; 65–84.
22. Pack, R. J., Al-Ugaily, L. H. and Morris, G. (1981) The cells of the tracheobronchial epithelium of the mouse: a quantitative light and electron microscope study. *J. Anat.* 132; 71–84.
23. Preston, G. M., Carroll, T. P., Guggino, W. B. and Agre, P. (1992) Appearance of water channels in Xenopus Oocytes expressing red cell CHIP28 protein. *Science* 256; 385–387.
24. Suzuki, T., Matsuzaki, T., Hagiwara, H., Aoki, T. and Takata, K. (2007) Recent advances in fluorescent labeling techniques for fluorescence microscopy. *Acta Histochem. Cytochem.* 40; 131–137.
25. Tajika, Y., Matsuzaki, T., Suzuki, T., Aoki, T., Hagiwara, H., Kuwahara, M., Sasaki, S. and Takata, K. (2004) Aquaporin-2 is retrieved to the apical storage compartment via early endosomes and phosphatidylinositol 3-kinase-dependent pathway. *Endocrinology* 145; 4375–4383.
26. Takata, K., Matsuzaki, T. and Tajika, Y. (2004) Aquaporins: water channel proteins of the cell membrane. *Prog. Histochem. Cytochem.* 39; 1–83.
27. Takata, K., Matsuzaki, T., Tajika, Y., Ablimit, A., Suzuki, T., Aoki, T. and Hagiwara, H. (2005) Aquaporin water channels in the kidney. *Acta Histochem. Cytochem.* 38; 199–207.
28. Tarran, R., Button, B. and Boucher, R. C. (2006) Regulation of normal and cystic fibrosis airway surface liquid volume by phasic shear stress. *Annu. Rev. Physiol.* 68; 543–561.
29. Yamashita, S. and Okada, Y. (2005) Application of heat-induced antigen retrieval to aldehyde-fixed fresh frozen sections. *J. Histochem. Cytochem.* 53; 1421–1432.